

# Tactile Sensing Based on Acoustic Resonance Tensor Cell

Hiroyuki SHINODA, Kenichi MATSUMOTO and Shigeru ANDO\*

Department of Electronic & Information Engineering,  
Tokyo University of Agriculture & Technology  
2-24-16 Koganei, Tokyo 184 Japan, shino@cc.tuat.ac.jp

\* Faculty of Engineering, University of Tokyo  
7-3-1 Hongo, Bunkyo-ku, Tokyo 113 Japan

## ABSTRACT

In this paper we propose a new tactile sensing element, acoustic resonant tensor cell. The structure is only a spherical cavity in an elastic tactile sensor body with two fine ultrasound paths extended respectively to an ultrasound transmitter and receiver which are placed at the bottom of the elastomer. The acoustic resonant frequency of the air in the cavity has an explicit relation with the principal stresses around it, which is easily detected by the ultrasound transducers. The sensor is simple and elastic. The single structure obtains useful tactile features of multi-dimensions. The principle and experimental results are described.

**Keywords:** Tactile sensor, Intelligent sensor, Artificial skin, Acoustic resonant tensor cell, 3-D structure.

## INTRODUCTION

In this paper we propose a new tactile sensing unit, Acoustic Resonant Tensor Cell, which senses the stress tensor in an elastic body. The structure is only a cavity ('spherical' in this paper) in an elastic tactile sensor body with two fine ultrasound paths extended respectively to an ultrasound transmitter and receiver placed at the bottom of the elastomer. We will show the acoustic resonant frequency of the air in the spherical cavity has an explicit relation with the principal stresses around it, which is easily detected by the ultrasound transducers.

The tactile sensor based on the sensing unit can have prominent characteristics which were not found in the past sensors [1,2,3] as

- 1.Elasticity** : The sensor is elastic without any rigid parts and wires.
- 2.Toughness** : It will be tough for mechanical damages because it has no fragile wires and parts.
- 3.Freedom of placement** : The unit can be placed at any point in 3-D elastic body [4] without any loss of sensitivity, accuracy and convenience of fabrication.
- 4.Multi-dimensional sensitivity** : The single structure of the unit obtains multi-dimensional feature of the stress tensor around it with high accuracy by multiple resonant frequencies of the cavity.

We originally intended to use the architecture for a tensor cell tactile sensor element, based on a principle that the detected rank of stress tensor matrix in an elastic body corresponds to the dimension of contact area[5]. (Fig. 1.) However we expect this can be

applied to a force, torque and deformation sensor of a flexible actuator, as well as to measurement systems in ergonomic studies to obtain pressure distribution between a human body and an elastic object.

## BASIC PRINCIPLE

Suppose there is a cavity ('spherical' in Fig.2) in an elastic body from which two paths are extended to an ultrasonic transmitter and receiver placed at the bottom of the elastomer as shown in Fig.2. The shape of the path is arbitrary but it becomes narrow smoothly near its junction with the cavity so that the diameter is sufficiently smaller than the cavity. In general, the ultrasound from the transmitter can hardly pass through the cavity to the receiver because of the acoustic impedance mismatching at the junction. But only at a resonant frequency determined by the cavity shape, the sound is transmitted through the

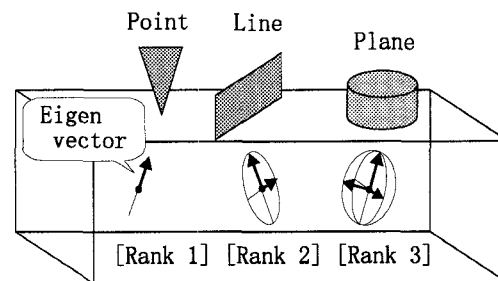


Fig. 1: Rank of stress tensor vs. contact dimension.

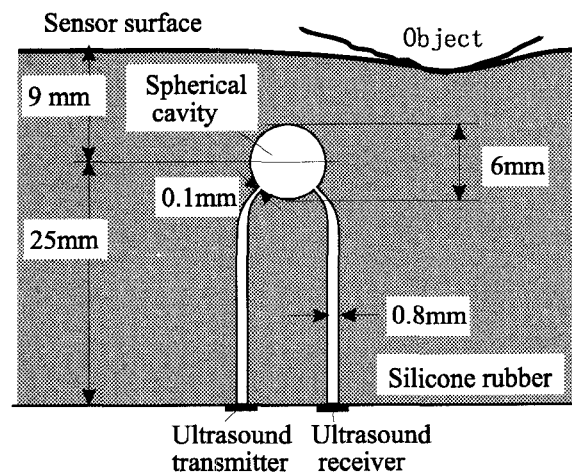


Fig.2: The structure of an acoustic resonant tensor cell.

cavity. ( If there were no viscous and molecular acoustic loss, the way of transmission would be the same with that by the direct connection between the two paths. ) Therefore we can know the resonant frequencies of the cavity by detecting peak frequencies of the acoustic transfer property. Here we must note that the peak frequency of the transmission hardly depends on the shape of the 'path', because the viscosity of the air in the fine long path prevents multiple reflections in it.

The next problem is the design of the cavity shape for obtaining useful tactile feature from the resonant frequencies. In the next section, we will show the relation of the resonant frequencies vs. cavity deformation in case of a 'spherical' cavity.

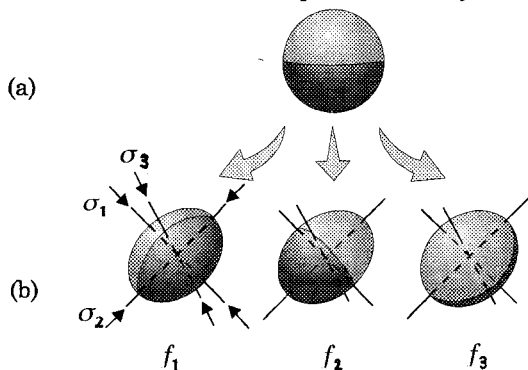


Fig.3: Phase maps of redundant resonant modes of the minimum resonant frequency before (a) and after (b) deformation.

RESONANCE IN A SPHERICAL CAVITY

We focus our attention on the acoustic resonance of the minimum resonant frequency in a spherical cavity. If we neglect the two paths, the resonant mode is expressed as

$$p(r, \theta, t) = f(r) \cos \theta e^{j\omega t} \tag{1}$$

by a polar  $r, \theta, \phi$  coordinate with an arbitrary direction and with the origin coinciding with the center of the sphere, where  $p$  is the sound pressure. Fig.3 (a) shows a resonant mode in which the air vibrates up and down mainly, with the pressure maximums at the top and the bottom of the sphere. The theoretical resonant frequency  $\omega_o$  for a cavity with a radius of  $r_o$  is given as  $\omega_o = 2.08 c / r_o$ , where  $c$  is the sound velocity.

Note that any direction of the vibration is allowed in case of true sphere.

Deformation vs. resonant frequencies

Suppose the sphere is slightly deformed into a ellipsoid by uniform stress around the cavity. (See Fig.3 (b).) Then the direction of the vibration which was arbitrary in a true sphere, is now allowed only along the three principal axes, and generally the

resonant frequencies  $f_1, f_2$  and  $f_3$  for each directional mode are different.

The ratios of the frequency changes to the original resonant frequency  $(\mu_1, \mu_2, \mu_3) =$

$(f_1 / f_o, f_2 / f_o, f_3 / f_o) - (1, 1, 1)$  are combined with the extension ratios of the sphere along the three principal axes  $(u_1, u_2, u_3)$  as

$$\begin{pmatrix} \mu_1 \\ \mu_2 \\ \mu_3 \end{pmatrix} = -\frac{1}{5} \begin{pmatrix} 3 & 1 & 1 \\ & 3 & 1 \\ * & & 3 \end{pmatrix} \begin{pmatrix} u_1 \\ u_2 \\ u_3 \end{pmatrix} \tag{2}$$

which is calculated by the perturbation technique[6].

Stress vs. cavity deformation

Elasticity theory gives the relation between uniform stress around the cavity and the cavity's extension ratios as [7]

$$\begin{pmatrix} u_1 \\ u_2 \\ u_3 \end{pmatrix} = \frac{3(1-\nu)}{2E(7-5\nu)} \begin{pmatrix} 9+5\nu & -1-5\nu & -1-5\nu \\ & 9+5\nu & -1-5\nu \\ * & & 9+5\nu \end{pmatrix} \begin{pmatrix} \sigma_1 \\ \sigma_2 \\ \sigma_3 \end{pmatrix} \tag{3}$$

where  $(\sigma_1, \sigma_2, \sigma_3)$  are principal stresses. (Principal stress is stress along the principal axis i.e. eigen value of stress tensor matrix.) Therefore the resonant frequency changes are combined with  $(\sigma_1, \sigma_2, \sigma_3)$  as

$$\begin{pmatrix} \mu_1 \\ \mu_2 \\ \mu_3 \end{pmatrix} = -\frac{3(1-\nu)}{2E(7-5\nu)} \begin{pmatrix} 5+\nu & 1-3\nu & 1-3\nu \\ & 5+\nu & 1-3\nu \\ * & & 5+\nu \end{pmatrix} \begin{pmatrix} \sigma_1 \\ \sigma_2 \\ \sigma_3 \end{pmatrix} \tag{4}$$

where  $E$  is Young's modulus and  $\nu$  is Poisson's ratio. The inverse of the transform always stable as

$$\begin{pmatrix} \sigma_1 \\ \sigma_2 \\ \sigma_3 \end{pmatrix} = -\frac{E}{6(1-\nu^2)} \begin{pmatrix} 6-2\nu & 3\nu-1 & 3\nu-1 \\ & 6-2\nu & 3\nu-1 \\ * & & 6-2\nu \end{pmatrix} \begin{pmatrix} \mu_1 \\ \mu_2 \\ \mu_3 \end{pmatrix} \tag{5}$$

if  $\nu \approx 0.5$ .

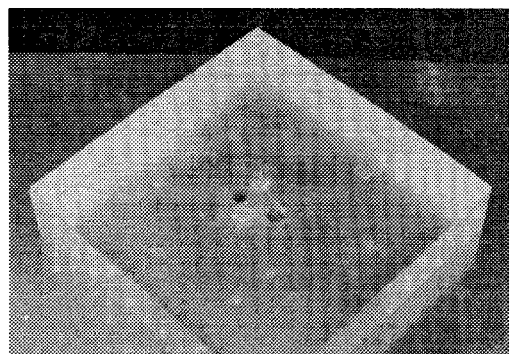


Fig. 4: Photograph of a 10cm x 10cm x 3cm silicone rubber with an acoustic resonant tensor cell.

FABRICATION AND EXPERIMENTS

We fabricated a tensor cell with a radius of 3mm in transparent silicone rubber ( Shin-Etsu KE-1935 ) as

shown in Fig. 4. Fig. 5 shows the transfer property of ultrasound from the transmitter to the receiver when nothing touches the sensor. A sharp peak was observed at theoretical resonant frequency of 38 kHz. The quality factor  $Q$  is realized as about 130.

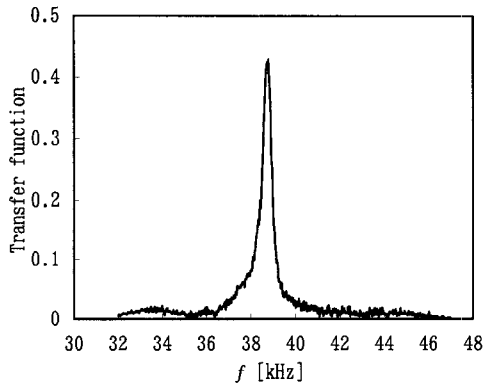
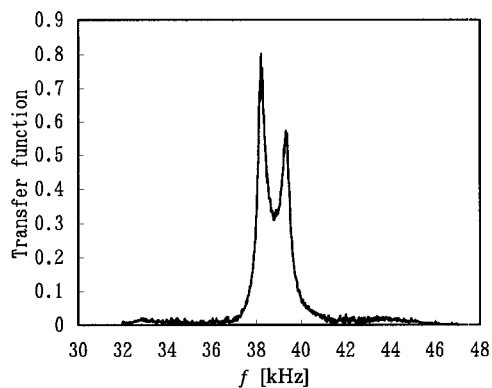
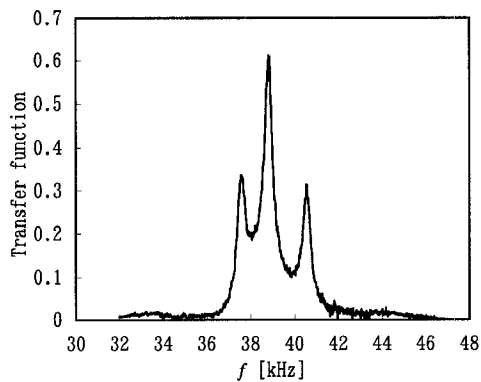


Fig. 5: Acoustic transfer function from the ultrasonic transmitter to the receiver through the cavity.



(a)



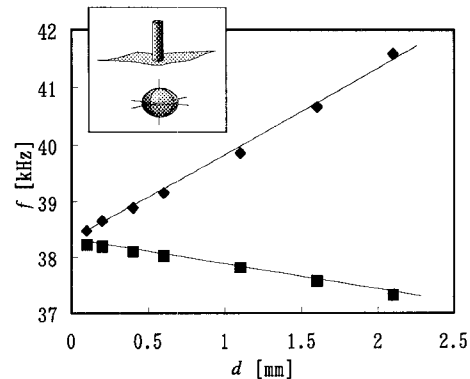
(b)

Fig. 6: Acoustic transfer functions from the transmitter input to the receiver output under point contact by a cylinder 3mm in diameter (a) and line contact (b).

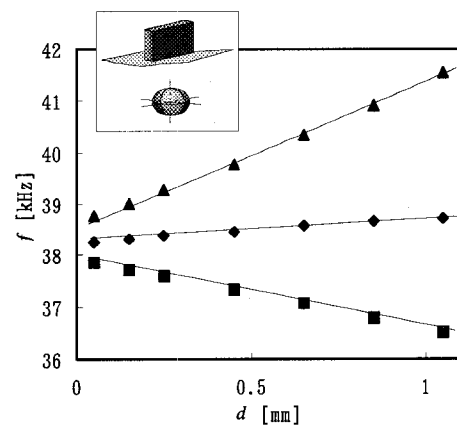
### Split of resonant frequency

The transfer property in Fig. 6 (a) is when a point ( a cylinder 3mm in diameter ) is pressed by 0.5mm on the sensor surface. The peak of the spectrum splits into

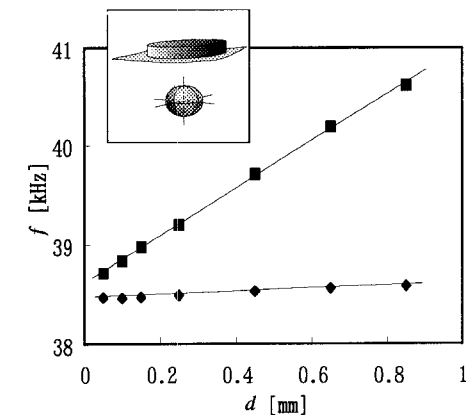
two because of the frequency difference between the vertical and the horizontal modes. ( We call a resonant mode with the vertical symmetrical axis 'vertical mode.' ) In case of line pressing, the modes split into three as shown in Fig. 6 (b).



(a)



(b)



(c)

Fig. 7: Resonant frequencies  $f$  vs. pressing depth  $d$  of three kinds of objects. Point contact (a), line contact (b) and plane contact by a disc 5cm in diameter (c).

Fig. 7 shows the relation between the resonant frequencies and pressing depth  $d$  of three typical kinds of objects. First, while a point ( a cylinder 3 mm in diameter ) was pushing the surface, the resonant frequencies began to split, and the interval of the peaks became wider linearly. (See Fig. 7 (a).) Because the cavity was compressed vertically, ( along the line

running through the contact point and the cavity, ) the vertical mode's resonant frequency increased while horizontal ones decreased. Next, Fig. 7 (b) shows the case of line contact. In this case, the resonant frequency of the vertical mode increases while that of one of two horizontal modes ( which vibrates perpendicular to the plane including the contact line and the tensor cell ) decreases, and the other one changes between the two. Finally, Fig. 7 ( c ) shows the plots of a disc pressing with a radius of 5 cm. All the modes have upward tendency.

**Detection of principal stresses**

Then we obtained Fig. 8 (b) by mapping measured principal stresses to a space whose horizontal and vertical axes express the ratio of the second to the major principal stress and the ratio of the third to the major, respectively. The inversion from the resonant frequency change to the principal stress was done by an experimental equation as

$$\begin{pmatrix} -\sigma_1 / E \\ -\sigma_2 / E \\ -\sigma_3 / E \end{pmatrix} = \begin{pmatrix} 1.0 & 0.41 & 0.41 \\ & 1.0 & 0.41 \\ * & & 1.0 \end{pmatrix} \begin{pmatrix} \mu_1 \\ \mu_2 \\ \mu_3 \end{pmatrix} \quad (6)$$

in place of Eq. (5), since the size of the cavity is not zero. The results demonstrate a fundamental property that the number of non-zero eigen values of stress tensor ( non-zero principal stresses ) i.e. the ranks of stress tensor matrix are 1, 2 and 3 for a point contact, a line contact and a plane contact, respectively. Here the experiments were done for the three kinds of object pressed at various locations as in Fig. 8 (a). The dispersion of the plots is owing mainly to the inaccuracy of Eq. (6) for the force not normal or not just above the cavity.

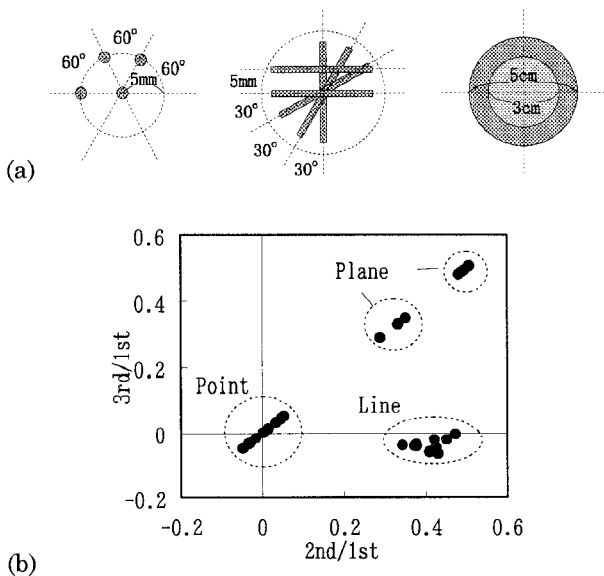


Fig. 8 : Detected eigen structures of stress tensor matrix for three kinds of contact types : point, line, plane. Plots to a space spanned by ratios of 2nd and 3rd principal stresses to the major principal stress.

**Detection of the change of contact area**

Fig. 9 shows the measured principal stresses vs. the pressing depth of a sphere with a radius of about 10 cm. It is seen that the ratio of the second principal stress to the major one increases according to the pressing depth. The result show that the single cell can detect the change of the contact area between the sensor and an object which gives the curvature of the object.

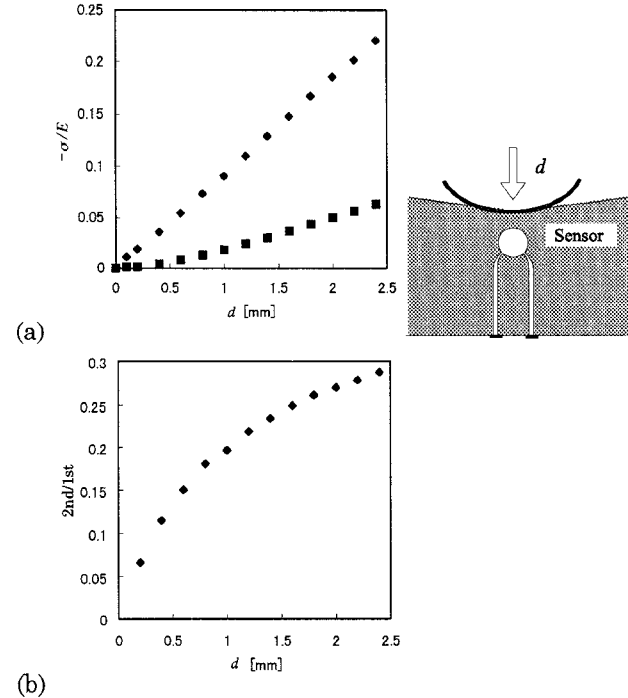


Fig. 9 : Measured principal stresses vs. pressing depth  $d$  of a sphere with a radius of about 10cm (a). The plots of the ratios of the measured principal stresses (b).

**REFERENCES**

- [1] H. R. Nicholls and M. H. Lee, "A Survey of Robot Tactile sensing Technology," *Int. J. Robotics Res.*, Vol. 8, No.3, pp.3-30, 1989.
- [2] P. P .L. Regtien, "Tactile Imaging," *Sensors and Actuators A*, Vol. 31, pp.83-39, 1992.
- [3] R. D. Howe, "Tactile Sensing and Control of Robotic Manipulation," *Journal of Advanced Robotics*, Vol. 8, No. 3, pp.245-261, 1994.
- [4] H. Shinoda, M. Uehara and S. Ando, "A Tactile Sensor Using Three-Dimensional Structure," *Proc. 1993 IEEE Int. Conf. Robotics and Automation*, pp.435-441, 1993.
- [5] H. Shinoda, N. Morimoto and S. Ando, "Tactile Sensing Using Tensor Cell," *Proc. 1995 IEEE Int. Conf. Robotics and Automation*, pp. 825-830, 1995.
- [6] A. Messiah, "Mécannique Quantique," Dunod, Paris, 1959.
- [7] S. P. Timoshenko and J. N. Goodier, "Theory of Elasticity," McGraw Hill, 1970.